Analyst

ROYAL SOCIETY OF CHEMISTRY

PAPER

View Article Online
View Journal | View Issue

Cite this: *Analyst*, 2022, **147**, 3470

Design of a photoelectrochemical lab-on-a-chip immunosensor based on enzymatic production of quantum dots *in situ*†

Beatriz Díez-Buitrago,[a,b] Francisco Javier Fernández-San Argimiro,[b] Jaione Lorenzo,[b] Goran Bijelic,[b] Nerea Briz[b] and Valeri Pavlov *[a]

In this work we report the development and validation of a photoelectrochemical immunosensor on the basis of alkaline phosphatase (ALP)-linked immunoassay for the detection of human serum albumin as a model analyte. In this biosensor, oriented immobilization of capture antibodies on aminated polystyrene was achieved *via* physical adsorption. After the interaction with the analyte, ALP immobilised on the surface through the sandwich immunoassay catalyses the hydrolysis of sodium thiophosphate (TP) to hydrogen sulphide (H_2S) which in the presence of cadmium ions yields CdS quantum dots (QDs). The electrical current is generated in the course of the photoelectrochemical process (PEC) during irradiation of the CdS QDs with a UV LED (365 nm) on home-made screen-printed carbon electrodes modified with a conductive polymer. Reaction time, steps and volumes were optimized for the miniaturization of the process in order to develop a lab-on-a-chip platform. The microfluidic system was designed with optimised parameters to fabricate the immunosensor combining the immunoassay with PEC detection. The final system presents a sensitivity comparable to that of the commercial kit thanks to the signal amplification enabled by the enzymatic growth of CdS QDs *in situ*. This photoelectrochemical immunosensing strategy potentially opens up a new avenue for the detection of a wide range of analytes of interest due to the universal and effective enzymatic signal amplification method. Moreover, the developed bioanalytical device allows for a great reduction of time and reagents compared to exiting commercial assays, making it suitable for point-of-care applications.

Received 30th September 2020,
Accepted 15th April 2022

DOI: 10.1039/d0an01950j

rsc.li/analyst

Introduction

In the last few decades the need for cheap, fast, and easy to use analytical tools has attracted increased attention for the development of portable biosensors for the qualitative and quantitative determination of different analytes in environmental, clinical, agricultural, food, and security and defence applications.[1–3] Biosensors have attracted much interest because of their features that include high sensitivity, specificity, ease of integration with other devices and portability for utilization at the point of use. Among the different biosensors on the market, immunosensors have demonstrated to be a valuable tool for rapid detection of a wide variety of target analytes with enhanced sensitivity and selectivity.[1,4–6] Despite the fact that a large number of immunoassays has been developed in research laboratories, bringing miniaturized portable devices for rapid detection to the market is very difficult. The complexity of the process and the need for expensive detectors hinder their integration into portable devices and encourage seeking new alternatives to address those drawbacks.

Immunosensors are based on the specific interaction between the antibody and the corresponding antigen leading to the formation of a stable complex. Transduction of this biorecognition event results in a change of some physical properties that can be transformed into a measurable electrical signal. Depending on the transducer and the detector, the immunosensors can use optical, thermal, piezoelectric or electrochemical transduction. Electrochemical biosensors have been the most successfully and widely used in the biomedical field and most areas of analytical chemistry due to their simplicity, short response time, facile miniaturization and relatively low cost.[6,7] Moreover, the biological recognition process provides high sensitivity and selectivity. Electrochemical biosensors offer some advantages over classical optical tech-

[a]*Center for Cooperative Research in Biomaterials (CIC biomaGUNE), Basque Research and Technology Alliance (BRTA), Paseo de Miramon 182, 20014 Donostia San Sebastián, Spain. E-mail: vpavlov@cicbiomagune.es; Tel: +34 943 00 53 08*
[b]*Tecnalia, Basque Research and Technology Alliance (BRTA), Paseo Mikeletegi 2, 20009 Donostia-San Sebastián, Spain*

† Electronic supplementary information (ESI) available. See DOI: https://doi.org/10.1039/d0an01950j

niques such as the ability to directly perform electrical signal processing, higher signal-to-noise ratio, elimination of optical interferences and no need for expensive external equipment.[8] Consequently, electrochemical transducers are suitable for construction of on-site detection devices. Photoelectrochemistry (PEC) is a promising technique that has gradually become a widespread analytical technique applicable to bioanalytical assays. PEC offers inherent high sensitivity of electrochemical procedures and the possibility of signal amplification with the suppression of the background signal thanks to the independent optical input signal and electrochemical output signal.[9,10] So far, most of the PEC immunoassays based on the amplified signal strategy are enzyme-labelled immunoassays.[11,12] In these analytical tests the detection antibody is labelled with a natural enzyme such as HRP[13,14] or ALP[15] that is able to catalyze the formation of a particular product that is subsequently used to trigger the PEC response.

The combination of signal amplification strategies with electrochemical methods (*e.g.*, PEC) has recently gained considerable attention because it allows the development of high-performance analytical tools for the ultrasensitive detection of trace amounts of a wide variety of analytes. Currently, point-of-use devices are compact systems with performance comparable to that of the laboratory tests which can be utilized by users with limited technical background. Furthermore, some requirements such as portability and automatization are essential in the design of new systems. The combination of microfluidic systems with biosensing devices resulted in the advent of laboratory-on-a-chip (LOC) technology that has demonstrated to be a key strategy to meet most analytical needs.[2,16] The integration of biosensors with microfluidic systems yields cost-effective miniaturized devices which are easy to handle. Miniaturization reduces volumes, dimensions and response time achieving better sensibilities and allows for the detection of different analytes on the same platform. The movement of fluidics can be precisely controlled electronically by pumps, valves or mixers[17] through a software, or manually by using syringes or blisters.[18] Miniaturization also makes the system more cost-effective because it utilizes batch fabrication manufacturing processes and requires only small volumes of potentially expensive reagents. Additionally, screen-printing methods provide a cost-effective and easy to scale technology to convert electrochemical biosensors into point-of-care devices.[19–21]

The aim of this work is to design, fabricate, characterize and validate an integrated platform for the development of a photoelectrochemical immunosensor. The proposed system is based on the enzymatic growth of CdS QDs *in situ* and their subsequent photoelectrochemical detection on a screen-printed carbon electrode. The immunoassay was optimised by ordered immobilization of antibodies on aminated polystyrene, reduction of the reaction steps, incubation time and injected volumes. The amplification of the signal was achieved with the photoelectrochemical procedure coupled to the enzymatic reaction of the immunoassay. Moreover, we designed and fabricated the screen-printed carbon electrodes and integrated them into the microfluidic system. The presented device showed a good performance and sensitivity comparable to that of a commercial kit for human serum albumin ELISA assay. Finally, it is important to highlight the great advantage that this system presents due to the possibility of application to any kind of immunoassay employing enzymatic amplification based on ALP.

Experimental

Materials

Alkaline phosphatase (ALP) from bovine intestinal mucosa, magnesium chloride ($MgCl_2$), sodium thiophosphate (TP), cadmium nitrate ($Cd(NO_3)_2$), 1-thioglycerol (TG), Trizma® base and hydrochloric acid (HCl) were obtained from Sigma. All water used was Milli-Q ultrapure grade. The electroconductive polymer was obtained by interaction of poly(vinylpyridine) with osmium ions (Os-PVP) according to the literature procedure.[22] Chlorosulfonic acid ($HClSO_3$) and sulfuric acid (H_2SO_4) were acquired from Panreac. Polystyrene 96-well plates were purchased from Falcon. Transparent polystyrene sheets of 190 μm and 1.2 mm thickness were purchased from GoodFellow (England). Conductive inks and insulating paste were acquired from Henkel and the adhesive from KIWO, Inc. The human serum albumin detection ELISA set was purchased from R&D Systems.

Apparatus

Absorbance measurements were performed on a Synergy H1 microplate reader (BioTek) using transparent microwell plates at room temperature. Fluorescence measurements were performed on a Varioskan Flash microplate reader (Thermo Scientific) using black multi-well microplates at room temperature. The system was controlled using SkanIt Software 2.4.3. RE for Varioskan Flash. The electrochemical tests were performed on an Autolab electrochemical workstation (model PGSTAT204, Metrohm Autolab, The Netherlands) furnished with NOVA 2.1 software. Disposable screen-printed carbon electrodes (SPCEs) were purchased from DropSens (model DRP-110). Scanning electron microscopy (SEM) images were recorded on a FEG (Field Emission Gun) ESEM (Quanta 250, FEI), operated in the low vacuum mode. The beam voltage was set to 10 kV, and the spot size was 5. Three different UV light sources were employed: a compact UV illuminator Model UVLM-28 from EL Series UVB Lamp and two LEDs from Kingbright (ATS2012UV365 and ATDS3534UV365B). X-ray Photoelectron Spectroscopy (XPS) experiments were performed on a SPECS Sage HR 100 spectrometer with a non-monochromatic X-ray source (magnesium Kα line of 1253.6 eV energy and 251 W).

Methods

Enzymatic assay. Various amounts of ALP were incubated with TP (0.5 mM) in Tris-HCl buffer (50 mM, pH 9) containing $MgCl_2$ (1 mM). After that, $Cd(NO_3)_2$ (2.5 mM) and TG (20 mM)

were added to the samples. Finally, fluorescence or photoelectrochemical response were recorded.

Chlorosulfonation and modification of polystyrene substrates. The chlorosulfonation procedure was carried out following a previously developed protocol.[23–25] In a thermostable reactor, polystyrene films of 1 mm were immersed in chlorosulfonic acid at −10 °C. After 20 min the samples were taken out and washed with cold (−10 °C) concentrated sulfuric acid. Finally, they were washed in an ice/water mixture and dried at room temperature. Afterwards, chlorosulfonated substrates were brought into contact with 5 M aqueous diamine solution and reacted for 20 min at room temperature. After that, they were rinsed with water and dried at room temperature.

Electrode printing. The electrodes were printed on aminated polystyrene by a screen-printing technique. Silver ink (LOCTITE EDAG PF 050 E&C) was used for vias and interconnections; silver chloride ink (LOCTITE EDAG PE 409 E&C) was used for the pseudo-reference electrode (E_{ref}); and carbon ink (LOCTITE EDAG 965SS E&C) was used for the working and counter electrodes (E_w and E_c, respectively). Initially, the silver paste was printed onto the substrate and dried at 80 °C for 40 min. Afterwards, the carbon ink was printed with the shape of the respective electrodes and dried at 80 °C for 40 min. This step was repeated 3–5 times depending on the substrate. Finally, the connections were covered with an insulating layer (LOCTITE EDAG PF 455B E&C) leaving the active area of electrodes accessible.

Immunoassay. Human serum albumin (HSA) kit was used to evaluate the bioanalytical performance of the system. An aminated polystyrene substrate was used as the platform for the immunoassay and the bioassay was carried out following the protocol of the kit. The sandwich ELISA was coupled to enzymatic reaction catalysed by ALP resulting in the formation of CdS QDs detected by PEC.

Photoelectrochemical detection. Before beginning the PEC assays, the SPCEs were cleaned by cyclic voltammetry (CV) in a potential range from 0 to 0.6 V at 50 mV s^{-1} in citrate-phosphate buffer (pH 7.5). After that, the Os-PVP polymer (40 μL drop of 2 mg mL^{-1}) was electrodeposited by CV scanning (2 cycles at a scan rate of 50 mV s^{-1} and a potential range from 0 to 0.6 V).[26,27] Finally, the modified SPCEs were rinsed with water and dried under an argon atmosphere. For PEC measurements, a 40 μL drop of sample was deposited on the SPCE surface and illuminated with a UV light emitting at 365 nm while applying a constant potential of 0.3 V *vs.* Ag/AgCl. For PEC measurements with the chip, UV light was irradiated to the channels with a powerful UV LED at 365 nm.

Results and discussion

Characterization of screen-printed carbon electrodes

The investigation of the electrode surface texture was carried out using scanning electron microscopy (SEM) to evaluate the effect of the electrode surface properties on the electrochemical response. Commercial SPCEs presented a uniform carbon layer with numerous fractures probably due to the application of high temperature and long time for the curing of the ink (Fig. 1A and D). Defects and cracks increase the edge plane effect on the graphite surface with a faster electrochemical reaction rate, which results in enhanced electron transfer.[28] The home-made SPCE (190 μm and 1.2 mm thick) showed a rough structure with some gaps throughout the surface (Fig. 1B, E and C, F, respectively) typical for unpolished electrodes.[29] These features result in the increase of the electrode active surface area and thus higher recorded current intensities (Fig. S1†).

XPS measurements were used to analyse more precisely the chemical composition of the home-made electrodes. This spectroscopic technique can provide atomic composition information of the topmost surface layers of the scree-printed carbon electrodes. The relative chemical composition and XPS spectra show the similarities of the carbon electrodes in terms of the presence of O, C, Si and Cl in the ink. In home-made electrodes the presence of Si and Cl is slightly higher than in the commercial ink due to the lower curing temperature during the fabrication process.

The ferri/ferrocyanide redox couple was the redox system used for comparing the electrochemical behaviour of screen-printed electrodes. A comparison of cyclic voltammograms is presented in Fig. S1.† Shapes of the resulting cyclic voltammograms obtained from the SPCEs on polystyrene substrates are very similar to those recorded with a commercial SPCE. Moreover, the redox couple exhibited a reversible behaviour with well resolved and stable oxidation and reduction peaks recorded during at least 10 cycles with the SPCEs printed on polystyrene (data not shown).

According to Table S1,† peak separations increased from 76 mV for commercial SPCE to 156 mV for carbon electrodes screen-printed on PS 190 μm and 821 mV for those screen-printed on PS 1.2 mm, at scan rates ranging from 50 to 200 mV s^{-1}. In all cases, ΔE_p values were higher than 59 mV, as expected for the Nernstian one-electron transfer. These

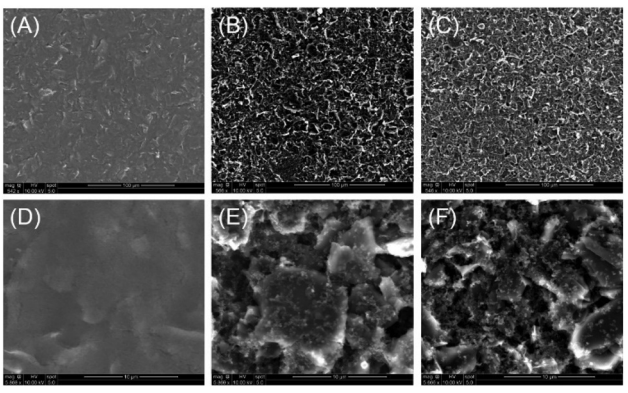

Fig. 1 SEM images of the commercial SPCE (A and D), and home-made SPCE on PS 190 μm (B and E) and PS 1.2 mm (C and F) with a magnification of 500× and 6000×, respectively.

results are typical for the heterogeneous process at the electrode materials caused by slower kinetics of partial electrode reactions. Nevertheless, the anodic/cathodic peak current (I_{ox}/I_{red}) ratio was always close to 1. A scan rate study of each electrode was performed for further characterization (Table S2†). Scan rate was varied from 50 to 200 mV s^{-1} and cyclic voltammograms were recorded (Fig. S1†). For all the electrodes a straight line was obtained in the plot of the peak currents *vs.* the square root of the scan rate. This linear relationship between the peak current density (both anodic and cathodic) and the square root of the scan rate demonstrated that the process was diffusion controlled. Parameters of the individual equations of the linear regressions (*k*: slope; *q*: intercept) with the corresponding correlation coefficient (R^2) are presented in Table S2.†

Optimization of experimental conditions

In order to apply the studied system to the development of a miniaturized device some requirements must be fulfilled. Volume of injected solutions, reagent concentration, incubation and reaction times should be optimized because they define the sensitivity and are the most important parameters to consider for miniaturization of the system. To produce a fast and reliable device we optimised the parameters regarding the photoelectrochemical detection (enzymatic reaction) and the immunoassay process with the aim of reducing time and volumes for further application in the miniaturized device.

Enzymatic reaction. Bovine ALP is widely used in bioanalysis as an enzymatic label in ELISA processes. ALP activity is routinely estimated by optical methods by using colorimetric substrates such as *para*-nitrophenylphosphate (pNPP) and fluorogenic ones like 4-methylumbelliferyl phosphate (4-MUP) coupled to expensive UV-vis or fluorogenic readers.[30,31] In this work, a standard potentiostat was used to detect the enzymatic activity by measuring the photoelectrochemical signal.

The mechanism of our enzymatic assay is based on biocatalytic hydrolysis of TP by ALP to orthophosphate (PO_4^{3-}) and H_2S. The latter reacts instantly with Cd^{2+} cations in Tris-HCl buffer generating CdS QDs stabilized by the buffer solution Trizma® base. The number of resulting CdS QDs is quantified photoelectrochemically by using modified carbon electrodes and a UV-illuminator source (Scheme 1). Carbon electrodes are modified with a conducting osmium polymer that "wires" the CdS QDs to the surface of the electrode when applying a positive voltage. The PEC signal is recorded after the application of 0.3 V (*vs.* pseudo reference electrode of Ag/AgCl) for 200 s and UV irradiation (365 nm) in the presence of TG that acts as redox mediator generating an electron flow through the CdS NPs to Os-PVP complexes and finally, the electrode.

The influence of the incubation temperature on the enzymatic activity is shown in Fig. 2A. The growth in photocurrent is directly related to the increase in the concentration of the enzyme in the studied range of bio-catalyst concentrations. According to PEC measurements, the activity of the enzyme is almost the same at room temperature (RT) and at 37 °C. It was decided to continue experiments at RT because portable and

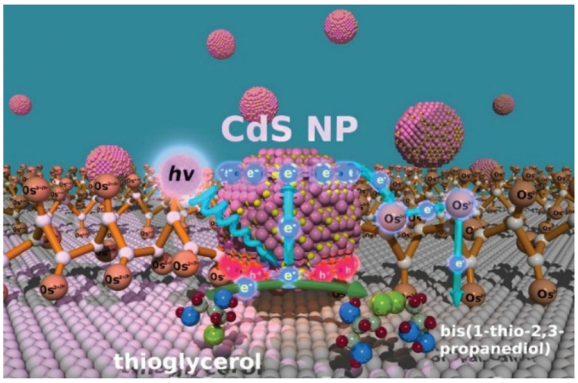

Scheme 1 Detection of CdS QDs on the screen-printed carbon electrode modified with an osmium polymer under UV irradiation.

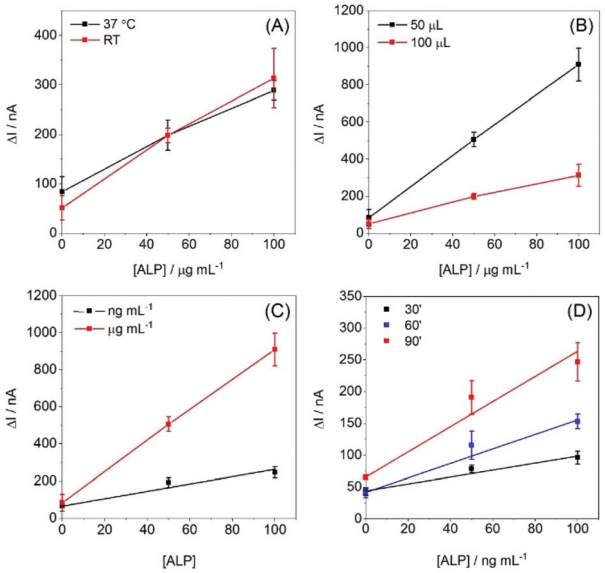

Fig. 2 Calibration plots reflecting the photocurrent response of CdS QDs in the system containing TP (0.5 mM), $Cd(NO_3)_2$ (2.5 mM), TG (20 mM) and variable ALP concentrations at (A) different temperatures, (B) different final volumes, (C) variable ALP concentrations at different ranges and (D) different TP incubation times.

point of care devices should be able to work under ambient conditions to simplify the operation of the device. We also evaluated the effect of different reaction volumes on the system response. The volume of the reaction mixture is an important parameter for adaptation of the enzymatic process to a microfluidic system regarding the homogeneity of the reaction mixture in terms of reagent diffusion. The enzymatic production of CdS NPs was carried out at two different reaction volumes of 100 and 50 μL (Fig. 2B). At these volumes the assay demonstrated a linear response up to 100 μg mL^{-1} of ALP and detection limits of 28 and 14 μg mL^{-1} for 100 and 50 μL, respectively, at a signal-to-noise ratio of 3 (S/N = 3). The decrease in volume to 50 μL improved the limit of detection by two times showing the same linearity as the process carried

out in a volume of 100 μL. These results confirmed the improvement of the analytical characteristics by reducing the reaction volume making it suitable for integration into a microfluidic system. Afterwards, the dependence of the photocurrent response on varying enzyme concentrations was studied. In ELISA tests the amount of the captured enzyme is usually very low, so a high signal/enzyme ratio is desired. In Fig. 2C it can be seen that a diminution of the PEC signal is observed when the enzyme concentration is decreased. Nevertheless, the linear response was still maintained as well as the detection limit, so it was concluded that this system could be used with small amounts of enzyme needed for the immunoassay. Finally, we evaluated the effect of the reaction time on the response value. The PEC response was determined after 30, 60 and 90 min of TP incubation as can be seen in Fig. 2D. These results demonstrate that the longer the incubation time, the more sensitive to ALP is the system. We selected 60 min as the best reaction time in order to achieve an agreement between sensitivity and reduced analysis time.

Considering the abovementioned experimental data, the following optimal parameters for the enzymatic generation of CdS NPs were selected: room temperature, 50 μL final volume and 60 min TP reaction time.

Immunoassay. Sandwich immunoassays were performed following the protocol of the ELISA kit for the detection of human serum albumin (HSA) at room temperature. In order to improve the immunoassay process, we studied the effect of reducing the number of steps and the incubation time of the assay. First, we evaluated the pre-incubation time of the antigen and the detection antibody prior to the interaction with the capture antibody immobilised on the aminated PS plate (Fig. 3A). The detection antibody was mixed with the antigen and allowed to react for a selected time. Next, the detection part of the ELISA protocol was followed which consisted of the determination of the biotinylated detection antibody using labelling with biotinylated HRP through streptavidin. The conversion of reduced TMB into the oxidised blue form of TMB was followed by UV-vis spectroscopy. Results obtained using shorter pre-incubation times were not significantly different from those obtained using the pre-incubation time recommended by the kit provider (2 h). Therefore, 5 min was established as the best pre-incubation time which showed similar results to that received according to the recommended procedure of the kit (2 h for this step).

Then, the effect of the incubation time with the capture antibody on the performance of the assay was studied (Fig. 3B). First, the enzyme ALP labelled with avidin was mixed with the biotinylated detection antibody to ensure antibody modification. Afterwards, the antigen was added and allowed to react for 5 minutes (step previously optimized). In order to detect the activity of ALP immobilised on the surface of the microplates, the fluorogenic substrate pNPP was employed. A decrease in the signal height was obtained when reducing the incubation time from 2 h (kit recommendation) to 5 min due to the rate of the biorecognition reaction. Despite the decrease in the signal, the slope didn't change dramatically which means that the system retains its sensitivity even at an incubation time of 5 min with the capture antibody. Nevertheless, in order to ensure a suitable sensitivity, 30 min incubation time with the capture antibody was selected for the following development of the PEC immunoassay.

From the results of this section it can be concluded that the immunoassay can be performed in a shorter incubation time in comparison with that of the regular standard ELISA kit. The new protocol allows reducing the volume and incubation time, two important features for designing a lab-on-a-chip, with performance similar to that of the commercial kit.

Analytical performance. We evaluated the analytical performance of the system with the optimised parameters using standard polystyrene microplates. The capture antibody was immobilised on the surface of aminated polystyrene microplates, then, the analyte was added and detected with the biotinylated detection antibody labelled with avidin–ALP conjugate. The enzymatic reaction to form CdS QDs was carried out in a final volume of 50 μL, at room temperature and using the abovementioned pre-incubation times of HSA with antibodies. PEC detection was conducted using an UV lamp emitting at 365 nm in the presence of 20 mM TG using home-made SPCEs modified with the osmium polymer. The photocurrent response corresponding to varying HSA concentrations (from 0 to 200 ng mL^{-1}) is depicted in Fig. 4A. The increase in the

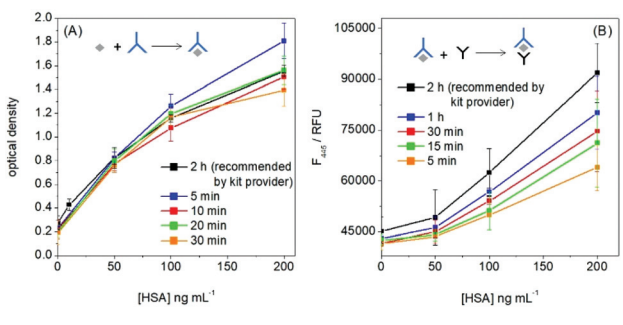

Fig. 3 (A) Calibration plot of the HSA ELISA assay at different pre-incubation times. (B) Calibration plot from HSA ELISA assay at different incubation times.

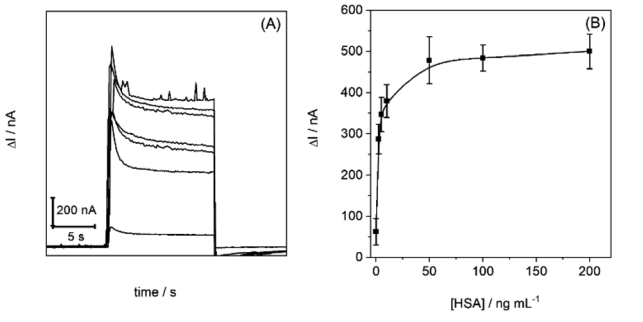

Fig. 4 (A) Photocurrent responses of the immunoassay recorded with the PS film SPCE and (B) calibration plot of the system based on CdS QD formation in a solution containing TP (0.5 mM), $Cd(NO_3)_2$ (2.5 mM), TG (20 mM) and variable HSA concentrations.

amount of HSA results in the increase of the observed photocurrent. Fig. 4B shows the calibration plot corresponding to different HSA concentrations. The curve demonstrated a linear response up to 10 ng mL^{-1}. The lowest amount of HSA that could be detected by this system was found to be 1.68 ng mL^{-1} (S/N = 3). This value is lower than that of the commercial kit (2 ng mL^{-1}) so it was confirmed that the photoelectrochemical process is suitable for the development of a photoelectrochemical immunosensor. The average relative standard deviation (RSD) calculated from the calibration plot was 7–11% (unless otherwise specified, RSD was always acquired utilizing no less than three independent measurements).

Chip design and fabrication

The design of the microfluidic device was performed considering the required steps of the immunoassay and the selection of the different optimised parameters mentioned above. As shown before, the assay consists of two processes: an ELISA immunoassay and the PEC detection. For this reason, the chip contains two chambers separated physically by a connector (Fig. S2†). The chamber for the ELISA immunoassay has an elongated shape to ensure the maximum reactive surface available during the assay with a standard width for the connectors. This design is important when working with microfluidics because the increase in the surface area to volume ratio allows for more efficient material transport.[32]

On the other hand, the chamber for PEC detection was round in order to cover the whole surface of the SPCE. The liquids are injected and evacuated manually with a syringe and the final volume was selected to be 50 μL so the height and width of the channels were calculated to meet all the requirements. The final microfluidic design pattern was drawn using SolidWorks modelling software. The dimensions of the channel for the immunoassay were 5 × 0.4 × 25 mm for width, height, and length, respectively and the chamber for PEC detection has a diameter of 8 mm and 0.4 mm height. A volume of 100 μL was selected for the reservoir which also acted as the inlet. The microfluidic channel was fabricated by ChipShop company (Germany) in polystyrene.

The fabrication of the bottom part was carried out taking into consideration the design of the microfluidic channels. The electrodes were printed on aminated PS as substrate following the procedure described above. The SPCEs consisted of a round working carbon electrode with a diameter of 4 mm surrounded by a counter (carbon) and a reference (Ag/AgCl) electrode. The width of the electrode is 8 mm (Fig. S3†).

A picture of the integrated device is shown in Fig. 5. The sealing of the channels to the electrode base was achieved with a suitable adhesive (KIWOPRINT® TC 2500). This is a high-quality pressure sensitive adhesive that is screen-printed on top of the polystyrene substrate allowing the sticking of both parts with high strength and stability.

Analytical validation

The validation of the final prototype was assessed by measuring the photocurrent response to increasing concentrations of HSA. Regarding the chip design (Scheme 2) the immunoassay is carried out in the aminated PS chamber, modified with capture antibodies, by injecting and removing the reagents through the inlet and outlet 1, respectively. During this process outlet 2 is kept closed. Second, the enzymatic growth of CdS QDs is carried out in the PS chamber. Finally, outlet 1 is closed and outlet 2 is left free in order to transfer generated CdS QDs from the PS chamber to the PEC chamber. The latter is used for PEC detection of enzymatically produced CdS QDs. The procedure is described in Fig. 6.

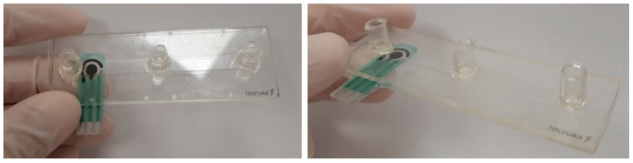

Fig. 5 Assembled microfluidic device used as a biosensor module. The device consists of an aminated PS substrate sealed with the PS microchannels that provide a connection to the mac-world (1 inlet port and 2 outlet ports).

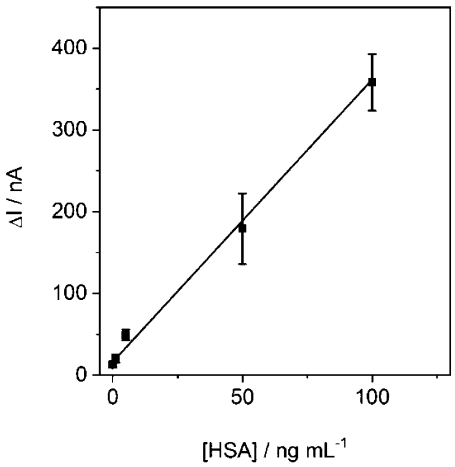

Scheme 2 Operation of the photoelectrochemical immunoassay based on the microfluidic device.

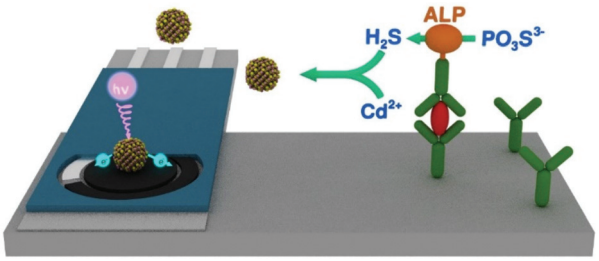

Fig. 6 Calibration plot of photocurrent by CdS QDs *vs.* HSA concentrations. The system contained TP (0.5 mM), $Cd(NO_3)_2$ (2.5 mM), TG (20 mM) and variable HSA concentrations with the SPCE printed on PS (1.2 mm) and the new microfluidic system, $\Delta I = 3.46 \cdot [HSA] + 15.93$.

Improved parameters from previous studies were used to perform this experiment: incubation at room temperature, 50 μL of sample solution, antibody labelling with ALP, pre-incubation with antigen and reduced assay time. The new protocol can be described as follows. First, capture antibody was immobilized on the aminated PS surface overnight at room temperature (2 μg mL^{-1}). After that, the surface was blocked with BSA 1% in PBS for 1 h. Subsequently, detection antibodies were labelled with ALP for 1 h prior to incubation with the antigen (5 min). Afterwards, the antibody–antigen complex was incubated in the channels with the capture antibody immobilized on the surface appropriately blocked to avoid non-specific interactions. Finally, the S^{2-} generated enzymatically by ALP from Na_3O_3PS interacted with Cd^{2+} to form CdS QDs. The photoelectrochemical signal was measured during irradiation of the electrode with a UV LED of 365 nm in the presence of 20 mM TG.

Previously several different methods for rapid *in situ* generation of QDs have been reported. For instance, luminescent water soluble glutathione coated CdTe QDs were synthesized.[33] The formation of CdTe QDs occurs spontaneously in the absence of any biocatalyst, hence this system is not suitable for enzymatic signal amplification. The synthesis of CdTe QDs controlled by chimeric DNA molecules ending up in the formation of the nanocrystals suitable for bioimaging has been described.[34] They are decorated with DNA aptamers and specifically bind to a number of targets. Employment of DNA-decorated CdTe QDs in amplified immunoassays is problematic, because the new QDs are not generated *in situ*. Another system based on the enzymatic reaction, in which *in situ* formation of fluorescent CdTe quantum dots (QDs) is blocked by butyrylcholinesterase has been published.[35] The higher the enzymatic activity the smaller the number of QDs generated, therefore application of this system to amplified immunoassays is not viable. A similar approach was recently reported[36] based on enzymatic blocking of growth of CdTe QDs. In this assay glucose oxidase generated hydrogen peroxide in the presence of glucose. Molecules of H_2O_2 oxidized L-cysteine to yield cystine, which does not stabilize the growth of CdTe QDs *in situ*, while in the absence of glucose L-cysteine remained intact promoting the growth of QDs. The optimum temperature for growth of CdTe QDs in that assay was 95 °C. Such harsh reaction conditions are not compatible with microfluidic devices.

The calibration plot obtained using the new microfluidic device is depicted in Fig. 6. It can be seen that the PEC signal increases gradually with HSA concentrations from 0 to 100 ng mL^{-1} due to the increased enzymatic growth of CdS QDs *in situ*. The curve exhibited a linear response in the range studied with R^2 of 0.996. Moreover, the detection limit was found to be of 1.97 ng mL^{-1}, comparable to that of the optical commercial kit (2 ng mL^{-1}). Besides, the average relative standard deviation (RSD) calculated from the calibration plot was 10–14% (unless otherwise specified, RSD was always acquired utilizing no less than three independent measurements). The standard ELISA kit required around 6 h per measurement while our device required only 2.5 h per measurement. Thus, this prototype demonstrated its feasibility for the development of a lab-on-a-chip device based on the photoelectrochemical detection system.

Conclusions

In summary, we presented a new promising platform for a photoelectrochemical lab-on-a-chip (LoC) immunosensor. Polystyrene substrates were modified to improve the antibody orientation and the sandwich immunoassay was coupled to the enzymatic growth of CdS QDs *in situ* for the subsequent measurement of the PEC response using home-made screen-printed carbon electrodes. The method showed an enhanced performance due to the improvement of the immunoassay and the signal amplification achieved with the enzymatic reaction. The miniaturization of the device comprised the design, optimization, characterization and validation of the system with a model analyte. The resulting platform showed an improved detection time and detection limit in comparison with those of the commercial ELISA kit for human serum albumin. The system developed in this study could be an attractive candidate for use with a wide range of analytes due to the versatility of the enzymatic signal amplification process and the broad range of possible functional groups that can be introduced on PS substrates for antibody immobilization. Moreover, the optimized protocol is fast, easy to use and convenient for point-of-care applications.

Conflicts of interest

There are no conflicts to declare. The manuscript was written through contributions of all authors. All authors have given approval to the final version of the manuscript.

Acknowledgements

This work was supported by the Spanish Ministry of Science, Innovation and Universities/AEI/FEDER, UE (RETOS I + D – Grant No. BIO2017-88030-R) and the Maria de Maeztu Units of Excellence Programme – Grant No. MDM-2017-0720, the Basque Government ELKARTEK program BMG17 and the Science, Technology and Innovation Gipuzkoa Program 2018. We thank Carolina Vera Martin for the design of the chip platform.

Notes and references

1 S. Andreescu and O. A. Sadik, *Pure Appl. Chem.*, 2004, **76**, 861–878.
2 G. Luka, A. Ahmadi, H. Najjaran, E. Alocilja, M. Derosa, K. Wolthers, A. Malki, H. Aziz, A. Althani and M. Hoorfar, *Sensors*, 2015, **15**, 30011–30031.

3 K. Yamanaka, M. C. Vestergaard and E. Tamiya, *Sensors*, 2016, **16**, 1–16.
4 T. Vo-Dihn, M. J. Sepaniak, G. D. Griffin and J. P. Alarie, *ImmunoMethods*, 1993, **3**, 85–92.
5 P. B. Luppa, L. J. Sokoll and D. W. Chan, *Clin. Chim. Acta*, 2001, **314**, 1–26.
6 F. S. Felix and L. Angnes, *Biosens. Bioelectron.*, 2018, **102**, 470–478.
7 E. B. Bahadir and M. K. Sezgintürk, *Anal. Biochem.*, 2015, **478**, 107–120.
8 C. Yang, Y. Huang, B. L. Hassler, R. M. Worden and A. J. Mason, *IEEE Trans. Biomed. Circuits Syst.*, 2009, **3**, 160–168.
9 A. Devadoss, P. Sudhagar, C. Terashima, K. Nakata and A. Fujishima, *J. Photochem. Photobiol., C*, 2015, **24**, 43–63.
10 W. W. Zhao, J. J. Xu and H. Y. Chen, *Chem. Soc. Rev.*, 2015, **44**, 729–741.
11 W. W. Zhao, Z. Y. Ma, P. P. Yu, X. Y. Dong, J. J. Xu and H. Y. Chen, *Anal. Chem.*, 2012, **84**, 917–923.
12 W. W. Zhao, Y. M. Han, Y. C. Zhu, N. Zhang, J. J. Xu and H. Y. Chen, *Anal. Chem.*, 2015, **87**, 5496–5499.
13 X. Zhang, M. Liu, Y. Mao, Y. Xu and S. Niu, *Biosens. Bioelectron.*, 2014, **59**, 21–27.
14 W. W. Zhao, X. Y. Dong, J. Wang, F. Y. Kong, J. J. Xu and H. Y. Chen, *Chem. Commun.*, 2012, **48**, 5253–5255.
15 B. Sun, F. Qiao, L. Chen, Z. Zhao, H. Yin and S. Ai, *Biosens. Bioelectron.*, 2014, **54**, 237–243.
16 L. Malic, D. Brassard, T. Veres and M. Tabrizian, *Lab Chip*, 2010, **10**, 418–431.
17 C.-Y. Lee, C.-L. Chang, Y.-N. Wang and L.-M. Fu, *Int. J. Mol. Sci.*, 2011, **12**, 3263–3287.
18 A. Disch, C. Mueller and H. Reinecke, in 2007 29th Annual International Conference of the IEEE Engineering in Medicine and Biology Society, 2007, pp. 6322–6325.
19 H. Dong, C.-M. Li, Y.-F. Zhang, X.-D. Cao and Y. Gan, *Lab Chip*, 2007, **7**, 1752–1758.
20 N. Godino, R. Gorkin, K. Bourke and J. Ducrée, *Lab Chip*, 2012, **12**, 3281–3284.
21 D. Zang, L. Ge, M. Yan, X. Song and J. Yu, *Chem. Commun.*, 2012, **48**, 4683–4685.
22 I. Katakis, L. Ye and A. Heller, *J. Am. Chem. Soc.*, 1994, **116**, 3617–3618.
23 A. Del Prado, N. Briz, R. Navarro, M. Pérez, A. Gallardo and H. Reinecke, *Macromolecules*, 2012, **45**, 2648–2653.
24 A. Del Prado, N. Briz, R. Navarro, M. Pérez, A. Gallardo and H. Reinecke, *Analyst*, 2012, **137**, 5666–5671.
25 A. Del Prado, N. Briz, R. Navarro, M. Pérez, A. Gallardo and H. Reinecke, *Vib. Spectrosc.*, 2013, **66**, 14–18.
26 J. Barroso, B. Díez-Buitrago, L. Saa, M. Möller, N. Briz and V. Pavlov, *Biosens. Bioelectron.*, 2018, **101**, 116–122.
27 J. Barroso, L. Saa, R. Grinyte and V. Pavlov, *Biosens. Bioelectron.*, 2016, **77**, 323–329.
28 K. K. Mistry, T. Sagarika Deepthy, C. R. Chaudhuri and H. Saha, *Curr. Sci.*, 2015, **109**, 1427–1436.
29 M. Yan, D. Zang, S. Ge, L. Ge and J. Yu, *Biosens. Bioelectron.*, 2012, **38**, 355–361.
30 J. Iqbal, *Anal. Biochem.*, 2011, **414**, 226–231.
31 N. Malashikhina, G. Garai-Ibabe and V. Pavlov, *Anal. Chem.*, 2013, **85**, 6866–6870.
32 A. Bange, H. B. Halsall and W. R. Heineman, *Biosens. Bioelectron.*, 2005, **20**, 2488–2503.
33 H. Quian, C. Dong, J. Weng and J. Ren, *Small*, 2006, **2**, 747–751.
34 N. Ma, E. H. Sargent and S. O. Kelley, *Nat. Nanotechnol.*, 2008, **4**, 121–125.
35 W. Deng, P. Chen, P. Hu, Z. He, M. Zhang, X. Yuan and K. Huang, *Sens. Actuators, B*, 2019, **292**, 180–186.
36 P. Hu, R. Zhou, D. Wang, H. Luo, X. Xiong, K. Huang, L. Li and P. Chen, *Sens. Actuators, B*, 2020, **308**, 127702.